Organic Electronics 50 (2017) 403–410

Contents lists available at ScienceDirect

Organic Electronics

journal homepage: www.elsevier.com/locate/orgel

Plasmonically enhanced lasing by different size silver nanoparticles-silver film hybrid structure

Shuya Ning [a], Zhaoxin Wu [b, *], Naming Zhang [c], Lei Ding [a], Xun Hou [b], Fanghui Zhang [a]

[a] College of Electrical and Information Engineering, Shaanxi University of Science and Technology, Xi'an, 710021, PR China
[b] Key Laboratory of Photonics Technology for Information, School of Electronic and Information Engineering, Xi'an Jiaotong University, Xi'an, 710049, PR China
[c] School of Electrical Engineering, Xi'an Jiaotong University, Xi'an, 710049, PR China

ARTICLE INFO

Article history:
Received 23 May 2017
Received in revised form
27 July 2017
Accepted 16 August 2017
Available online 18 August 2017

Keywords:
Organic lasing
Localized surface plasmon resonance
Enhanced localized electric field
Multiple scattering

ABSTRACT

We reported on the enhanced lasing in organic dyes based on plasmonic hybrid structure of Ag nanoparticles (NPs)-Ag film, the diameters of Ag NPs ranged from 20 nm to 100 nm. The lowest lasing threshold was achieved by the optimal size Ag NPs-Ag film hybrid structure, which was reduced by 5.2 times than that of the neat gain medium. Comparing to the separate Ag NPs or Ag film, the hybrid structure presented the more intense local electric field due to the plasmonics coupling between the localized surface plasmons of Ag NPs and the surface plasmon polariton of Ag film, and the stronger scattering due to the reinjection of the leaking photons by external feedback of Ag film. The effects of different sizes Ag NPs-Ag film hybrid structures on lasing were investigated. It found that when the Ag NPs in hybrid structure is small (diameter≤40 nm), the enhanced localized electric field plays a major role on enhanced lasing; with the increase of Ag NPs size, the enhanced electric field and scattering have comparable contribution on enhancing lasing; for the larger size Ag NPs-Ag film (diameter≥80 nm), the scattering effect is the dominant mechanism for random lasing. Then the lowest threshold was dominated by the balance of enhanced localized electric field and scattering effect. Our results could provide us a unique idea to effectively enhance the lasing of organic dyes, and realize the lower pumped threshold and stronger lasing.

1. Introduction

Localized Surface Plasmons (LSPs) can be excited on metal nanoparticles (NPs) whereas delocalized surface plasmon polariton (SPP) can be excited on metallic film, which both can induce the field enhancement in the near-field region [1–4]. Various groups have already used metallic NPs to enhance lasing. For example, O. Popov et al. utilized gold NPs to enhance lasing from a polymer film doped with Rhodamine 6G [5,6]. X. Meng et al. achieved the enhanced emission of coherent random lasing in polymer films by introducing Ag NPs [7,8]. T. Zhai et al. demonstrated an enhanced random laser based on gold nano-island structures with a layer of dye-doped polymer [9]. E. Heydari et al. reported the emission enhancement for the gold NP-based waveguided random laser [10]. However, for the metallic film in planar waveguide structure, it would increase the lasing threshold duo to the quenching effect of metallic film on lasing of dyes, which is a major obstacle to obtain stimulated emission under electrical pumping [11,12]. Substantial efforts have been made to restore and optimize the optically pumped lasers in the presence of metallic film, such as polymer film deposited on distributed feedback metallic structure [13,14], adopting in low loss metal cladding [15–17], or introducing the spacer between polymer film and metallic film [18]. Despite all these attempts, it is still desired to further reduce the lasing threshold of optically pumped laser in the presence of metallic film.

Here, a particularly interesting plasmonic system which has received somewhat less attention, metallic NPs-metallic film hybrid structure was explored. We systematically investigated the effects of different sizes Ag NPs-Ag film hybrid structures on the lasing of gain medium, the diameters of Ag NPs ranged from 20 to 100 nm. The lowest lasing threshold of the gain medium deposited on 60 nm Ag NPs-Ag film hybrid structure was found, which greatly reduced 5.2 times than that of the gain medium deposited on glass. For comparing, the devices that gain medium deposited on Ag film,

* Corresponding author.
E-mail address: zhaoxinwu@mail.xjtu.edu.cn (Z. Wu).

http://dx.doi.org/10.1016/j.orgel.2017.08.018
1566-1199/

silver island film (SIF) were also prepared. It found that the Ag NPs-Ag film coupled system could better enhance lasing, which is because that the Ag NPs-Ag film hybrid structure presents the more intense local electric field due to the plasmonics interaction between LSPs of the Ag NPs and the SPP of Ag film, and the stronger scattering effect due to the re-injection of emitted light into the organic gain media of planar waveguide structure by the external feedback of Ag film.

At meanwhile, the effects of different sizes Ag NPs-Ag film hybrid structures on lasing properties were studied. It was noting that the enhanced localized electric field and scattering effect of Ag NPs-Ag film all work on the reduction of lasing threshold. However, according to the experiment and theoretical analysis, it was found that when the Ag NPs in hybrid structure is small (diameter≤40 nm), the enhanced localized electric field plays a more significant role on the enhanced lasing of organic dyes; with the increase of Ag NPs size for hybrid structure, the enhanced localized electric field and scattering play the comparable role on the lasing; when the Ag NPs size is larger (diameter≥80 nm), the scattering effect of Ag NPs-Ag film mainly contributes to the enhanced lasing. Then we concluded that the optimal size Ag NPs-Ag film could provide a balance between enhanced local electric field and scattering to realize maximum lasing. At meanwhile, the negative effect of metallic film is avoided to realize the lower pumped threshold than that of the metal-free device.

2. Experiment

2.1. Synthesis of different size Ag NPs

Different sizes Ag NPs were synthesized according to the seed-mediated growth method by citrate reduction of silver nitrate ($AgNO_3$) with $NaBH_4$ as strong reducing agent [19]. Firstly, small Ag NPs were synthesized under chemically reducing $AgNO_3$ in aqueous solution by a rapid nucleation-growth-ripening principle, the resulting Ag NPs were used as starter seeds. Then, slowly adding proper portions of Ag salt and citrate reducer into the starter seeds solution obtained in the first step. In this way, we prepared Ag NPs with diameters about: 20, 40, 60, 80, 100 nm.

2.2. The devices based on different sizes Ag NPs-Ag film hybrid structure

In order to systematically study the properties of different sizes Ag NPs-Ag film hybrid structures, we developed the devices that gain media deposited on different sizes Ag NPs-Ag film, the diameters of Ag NPs were about 20, 40, 60, 80, and 100 nm, respectively. The device structures were Glass/Ag film (50 nm)/SiO_2 (10 nm)/Ag NPs/LiF (5 nm)/PS:BMT-TPD (shown in Fig. 1). For comparison, the gain medium deposited on glass was also prepared as reference. The preparation process of devices was following manner:

Firstly, a continuous Ag film of thickness 50 nm was evaporated onto a glass substrate. The 10 nm-SiO_2 layer was radio frequency sputtered over the silver surface, which could serve to protect the metal surface from chemical attack, and to provide a means to chemically attach silver colloids. SIFs were deposited according to the procedure described elsewhere [20]. The Ag film coated with SIF was prepared. Fig. 2 shows the atomic force microscopy (AFM) images of the Ag NPs with different sizes.

Then the planar waveguide structures were fabricated. N,N′-bis(3-methylphenyl)-N,N′-diphenyl-[1,1':4′,1″-terphenyl] -4,4″-diamine (BMT-TPD) was used as gain medium [21]. Polystyrene (PS) and BMT-TPD were dissolved in chloroform solution (PS: BMT-TPD = 4:1, wt%). The gain medium films were obtained by spin coating the solutions onto LiF layers at speed 4000 rpm, and were annealed at 110 °C for 10 min to remove the solvent. The 5 nm-LiF layer was deposited over the SIF surface to prevent quenching caused by direct contact between Ag NPs and gain medium. The thickness of gain medium layer is approximately 250 nm.

2.3. Characterization

The absorption and photoluminescence (PL) spectra were

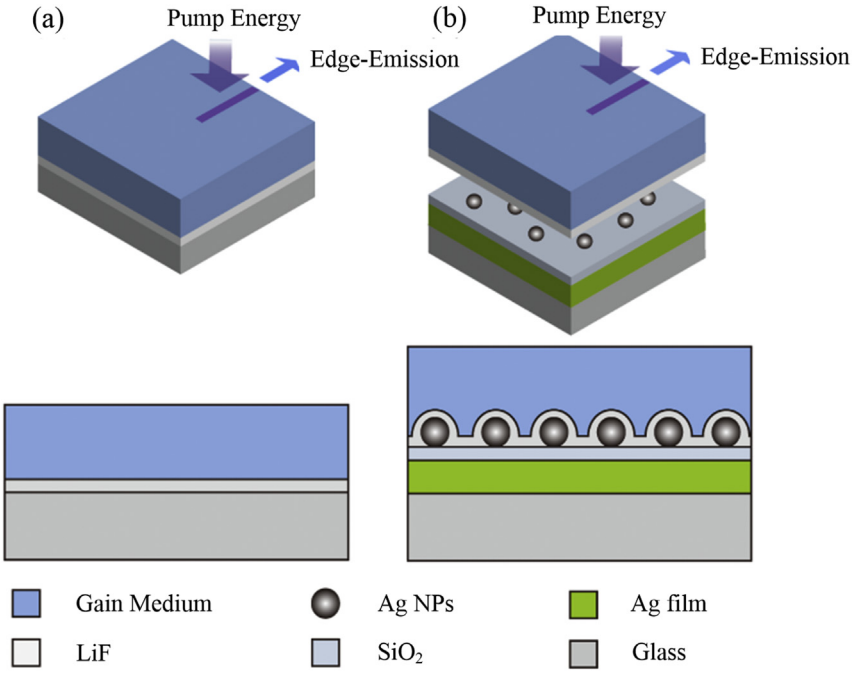

Fig. 1. The schematic illustrations of different devices. (a) Glass/LiF (5 nm)/PS:BMT-TPD (reference device); (b) Glass/Ag film (50 nm)/SiO_2 (10 nm)/Ag NPs/LiF (5 nm)/PS:BMT-TPD.

obtained by UV–Vis spectrophotometer (HITACHI U-3010, Japan) and Fluorescence Spectrometer (Fluoromax-4 spectrofluorometer). The thicknesses of polymer layers were measured with Stylus Profiler (Dektak 6M, USA). The devices were photopumped at normal incidence with a Nd: YAG laser (355 nm, 10 Hz repetition rate, and 5.5 ns pulse duration). An adjustable slit and a cylindrical lens were used to shape the beam into a stripe with the size of 7 mm × 1 mm. For the devices shown in Fig. 1, they present the waveguide scheme. When the devices are pumped, the light is partially confined into the waveguide and amplified by the gain medium as it is reflected (or scattered) by the internal surfaces of waveguide and propagates along the path of optical gain. As a result, the light emitted from the edge of the waveguide could undergo the longer light path and more gain process in gain medium, which leads the lower lasing threshold and stronger emission intensity according to the optical confinement of the waveguide. Therefore, the edge emission spectrum was measured to study the lasing properties of devices [22,23]. And The edge emission spectra were collected by Fiber Optic Spectrometer (Ocean Optics SpectraSuite, USB2000).

3. Results and discussion

Fig. 3 shows the localized surface-plasmon resonance (LSPR) bands of different sizes Ag NPs, together with the absorption and emission spectra of BMT-TPD. It exhibits that the LSPR peaks of these different sizes Ag NPs undergo a red shift from 410 to 449 nm as the diameters of Ag NPs range from 20 nm to 100 nm, which lead

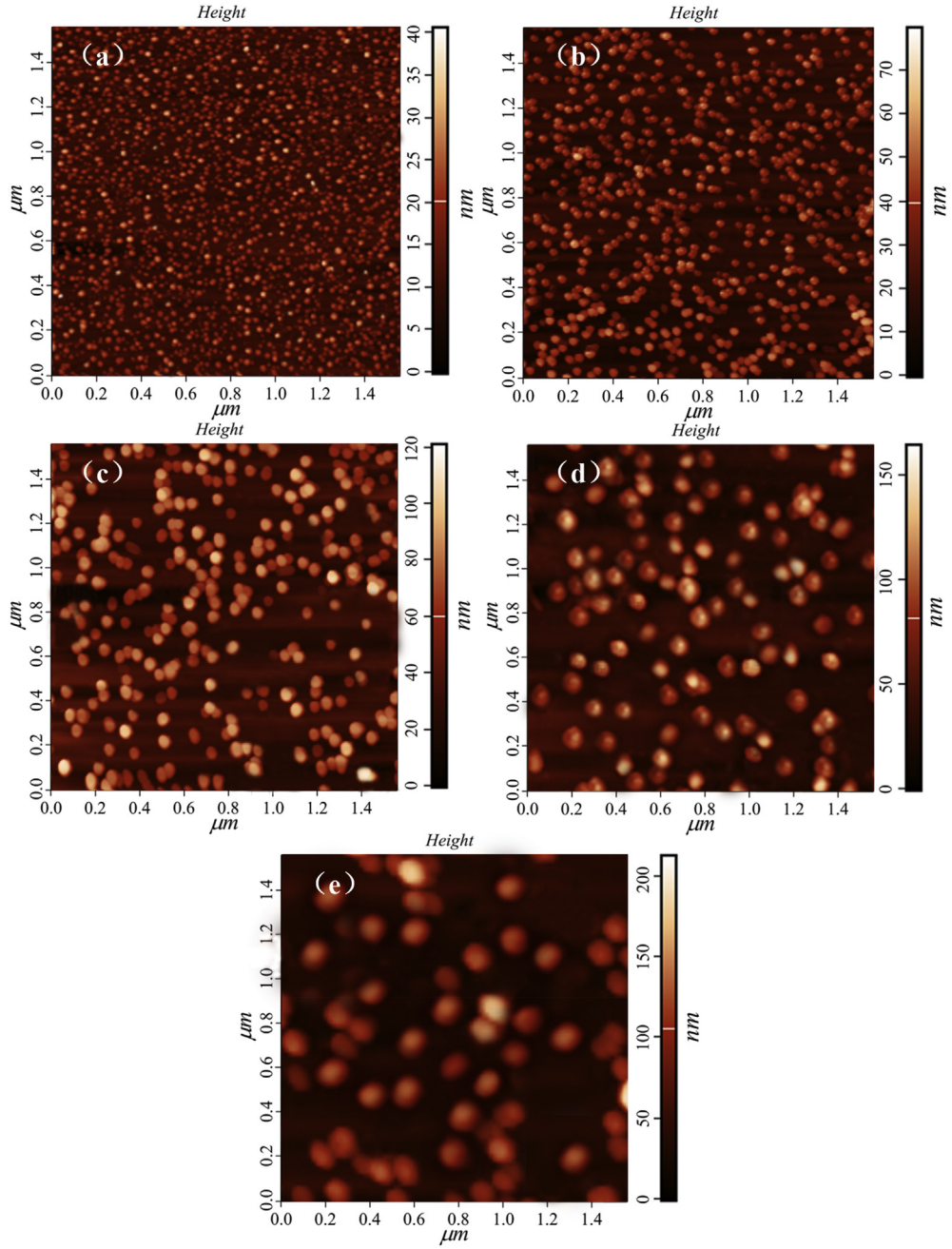

Fig. 2. The AFM images of different sizes Ag NPs, the diameters are about (a) 20 nm, (b) 40 nm, (c) 60 nm, (d) 80 nm, and (e) 100 nm.

the different effect on surface plasmon mediated emission enhancement.

For comparison, the device that gain medium deposited on glass was fabricated as reference (shown in Fig. 1(a)). Fig. 4(a) depicts the emission spectra of reference device at different pump intensities, which exhibits an obvious amplified spontaneous emission (ASE) behavior [24,25]. At first, the emission intensity increases slowly with the increase in pump intensity, the broad emission spectrum is shown. With further increase in the pump intensity, the emission spectrum becomes narrow with a steep increase of the emission intensity. The rapid decrease in linewidth of emission spectra above the threshold is shown in the inset of Fig. 4(a), which exhibits the threshold of 42.9 μJ/cm^2.

To investigate the effect of different sizes Ag NPs-Ag film hybrid structures on lasing properties, the different sizes Ag NPs-Ag film hybrid structures were introduced into the gain media (the device structure is shown in Fig. 1(b)) and the optimal size Ag NPs-Ag film hybrid structure was found. Fig. 4(b)-(d) show the emission spectra of devices that gain media deposited on Ag NPs-Ag film hybrid structures, the diameters of Ag NPs in hybrid structures are 20, 60 and 100 nm, respectively. The sharp spikes with full width at half maximum (FWHM) of about 1 nm are observed, which indicate the occurrence of coherent random lasing. For the waveguide-plasmonic scheme shown in Fig. 1(b), a large part of the scattered light may be totally reflected back at the gain medium/air interface to propagate within the waveguide and scattered further by the Ag NPs, then the scattered light is enhanced or amplified by the gain medium through the confinement of the scattered light into the waveguide. Therefore, the multiple scattering of Ag NPs and waveguide confinement mechanisms provide effective gain channels [9,26,27]. The random lasing could occur. The intensities and FWHMs of corresponding emission spectra are shown in the insert of Fig. 4(b)-(d). It shows that when the pump energy is higher than the lasing threshold, the emission intensity increases rapidly and the FWHM decreases to about 1 nm. Fig. 4(e) illustrates the emission intensity as a function of pump energy for devices that gain medium deposited on different sizes Ag NPs-Ag film hybrid structures, the Ag NPs diameters are 20, 40, 60, 80 and 100 nm, respectively. The corresponding lasing thresholds are exhibited in Fig. 4(f) and Table 1. It shows that with the increase of Ag NPs size, the lasing threshold exhibits a profound reduction at first, and turns to increase. The lowest lasing threshold of 8.3 μJ/cm^2 is found for the device with 60 nm Ag NPs-Ag film hybrid structure, about a factor of 5.2 times lower than that of neat gain medium.

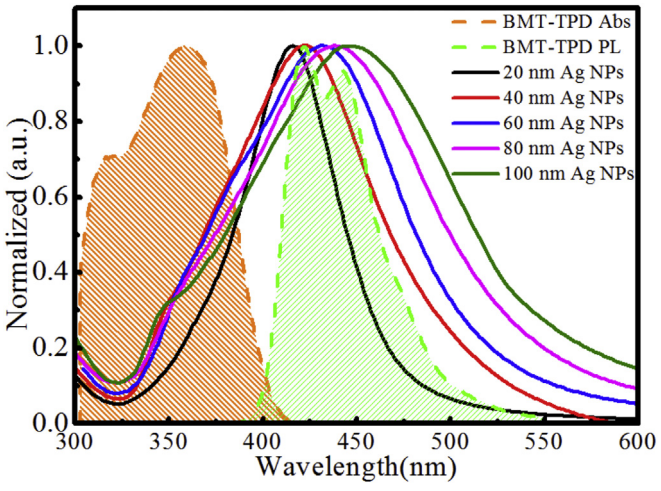

Fig. 3. The LSPR spectra of different sizes Ag NPs, together with the absorption and emission spectrum of BMT-TPD.

For further presenting the advantages of Ag NPs-Ag film hybrid structure on enhanced lasing, we developed the devices that gain media deposited on Ag film, SIFs, respectively, the corresponding device structures are Glass/Ag film (50 nm)/SiO_2 (10 nm)/LiF (5 nm)/PS:BMT-TPD, Glass/Ag NPs (60 nm)/LiF (5 nm)/PS:BMT-TPD, respectively. Fig. 5 (a)-(c) show the emission spectra of the devices that gain medium deposited on Ag film, 60 nm Ag NPs, and 60 nm Ag NPs-Ag film with 100 nm SiO_2 spacer, respectively. Fig. 5 (b) and (c) show the sharp spikes in emission spectra above the lasing threshold, which indicate the random lasing behaviors due to the existing of Ag NPs. Fig. 5(d) illustrates the emission intensity as a function of pump energy for the devices that gain medium deposited on glass, Ag film, 60 nm Ag NPs, 60 nm Ag NPs-Ag film with 100 nm and 10 nm SiO_2 spacers. The corresponding lasing thresholds are 42.9, 37.4, 28.3, 21.4 and 8.3 μJ/cm^2, respectively. We can find that the lasing thresholds of device based on Ag NPs-Ag film are lower than that based on other substrates, suggesting that the Ag NPs-Ag film hybrid structure could more effectively enhance the lasing properties than independent Ag NPs and Ag film. In addition, for the device with Ag NPs-Ag film hybrid structure, comparing to the Ag NPs-Ag film with 100 nm SiO_2 spacer, there is lower lasing threshold for that with 10 nm SiO_2, which indicates that the interaction of LSP and SPP plays the important role on enhanced lasing.

As we known, the metallic nanostructures are constantly used to enhance the lasing due to the both underlying mechanisms of enhanced localized electric field and enhanced scattering strength [6]. On the one hand, the enhanced localized electric field could increase pump light density and excitation rate, the more dye molecules could be excited to the higher energy levels. Meanwhile, the quantum yield and radiative decay rate of dye molecule could be increased. On the other hand, the metallic nanostructures could also scatter the emitter energy with the greater scattering strength, which could further enhance the lasing properties.

In order to determine which mechanism of hybrid structure takes effect on enhanced lasing properties, the devices based on different sizes Ag NPs-Ag film hybrid structures with 50 nm-LiF spacer between SIFs and gain media were prepared, the thickness of LiF spacer of device shown in Fig. 1(b) was changed to 50 nm [28]. For the device with 5 nm-thick LiF spacer, the quenching effect of dyes could be avoided, both the enhanced localized electric field and scattering of Ag NPs-Ag film contribute to enhanced lasing; and for the device with 50 nm-thick LiF spacer, the enhanced localized electric field effect of Ag NPs-Ag film is avoided, only the scattering effect of Ag NPs-Ag film hybrid structure works [28].

The lasing thresholds of devices with 5 nm or 50 nm LiF spacer layers between gain medium and SIFs are shown in Table 1. In Table 1, $E_{th\text{-}5nm}$ ($E_{th\text{-}50nm}$) is the lasing threshold of devices with 5 nm (50 nm) LiF spacer; E_{th} is the ASE threshold of reference device; D is the diameter of Ag NPs. $E_{th\text{-}5nm}/E_{th}$ ($E_{th\text{-}50nm}/E_{th}$) is the ratio of threshold for device with 5 nm (50 nm) LiF spacer and the reference device, which exhibits the degree of threshold reduction for the devices with 5 nm (50 nm) LiF spacer comparing to the reference device. $E_{th\text{-}5nm}/E_{th}$ reveals the contribution of both enhanced localized electric field and scattering effect of Ag NPs-Ag film hybrid structure on threshold reduction, and $E_{th\text{-}50nm}/E_{th}$ reflects the contribution of only scattering effect of corresponding Ag NPs-Ag film on reduced threshold.

In Table 1, it shows that the devices with 5 nm LiF spacer exhibit the superior performance and lower lasing threshold comparing to corresponding devices with 50 nm LiF spacer. And we found that the effects of enhanced localized electric field and scattering of hybrid structure all contribute to the reduced lasing threshold. When the Ag NPs is small in hybrid structure (the diameter of Ag

NPs≤40 nm), the enhanced localized electric field is the major mechanism to enhance lasing. For example, for the device with 40 nm Ag NPs-Ag film, the $E_{th\text{-}5nm}/E_{th}$~0.25, the corresponding $E_{th\text{-}50nm}/E_{th}$ ~0.74, suggests that comparing to the scattering effect of 40 nm Ag NPs-Ag film, the contribution of enhanced localized electric field of 40 nm Ag NPs-Ag film on the lasing can be more, which plays the main role on reducing lasing threshold. With the increase of Ag NPs size, the scattering effect is stronger, for the device with 60 nm Ag NPs-Ag film, the $E_{th\text{-}5nm}/E_{th}$~0.2, the corresponding $E_{th\text{-}50nm}/E_{th}$~0.62. It shows that the enhanced localized electric field and scattering have comparable contribution to enhance lasing. In the same way, when the size is larger in hybrid structure (the diameter of Ag NPs≥80 nm), such as device with 100 nm Ag NPs-Ag film, the $E_{th\text{-}5nm}/E_{th}$~0.33, the corresponding $E_{th\text{-}50nm}/E_{th}$~0.43, suggests that comparing to the enhanced localized electric field effect, the scattering effect of 100 nm Ag NPs-Ag film plays the main role on reducing lasing threshold.

In order to investigate the reason of experiment results above, two mechanisms of enhanced localized electric field and scattering are discussed respectively.

On the one hand, for the enhanced localized electric field of Ag NPs-Ag film hybrid structure. We know that the light can directly excite the LSPR of metallic NPs, but it cannot directly excite the SPP of metallic film due to the inherent wave vector mismatch between the SPP and the photons traveling in the air region. In the Ag NPs-Ag film hybrid structure, the Ag NPs could provide an indirect way to excite the SPPs of the Ag film by the diffraction effect, thus the SPP can be excited [3,4].

Table 1
The thresholds of devices with 5 nm or 50 nm LiF spacer layers between gain medium and SIFs. E_{th} is the ASE threshold of reference device; $E_{th\text{-}5nm}$, $E_{th\text{-}50nm}$ are the lasing threshold of devices with 5 nm or 50 nm LiF spacer; D is the diameter of Ag NPs. $E_{th\text{-}5nm}/E_{th}$ ($E_{th\text{-}50nm}/E_{th}$) is the ratio of lasing threshold for device with 5 nm (50 nm) LiF spacer and the reference device.

D (nm)	Device with 5 nm LiF spacer		Device with 50 nm LiF spacer	
	$E_{th\text{-}5nm}$ (μJ/cm^2)	$E_{th\text{-}5nm}/E_{th}$	$E_{th\text{-}50nm}$ (μJ/cm^2)	$E_{th\text{-}50nm}/E_{th}$
20	24.6 ± 0.98	0.57	36.5 ± 0.96	0.85
40	10.7 ± 0.91	0.25	31.8 ± 0.99	0.74
60	8.3 ± 1.18	0.2	26.6 ± 1.1	0.62
80	13.1 ± 1.36	0.31	22.9 ± 0.84	0.53
100	14.1 ± 1.1	0.33	18.6 ± 1.04	0.43

In order to investigate the localized electric field of different sizes Ag NPs-Ag film hybrid structures, the electric field intensity distributions of different sizes Ag NPs-Ag film hybrid structures were calculated using the COMSOL software. Fig. 6 (a)-(e) show the electric-field distribution of different sizes Ag NPs-Ag film hybrid structures with 10 nm SiO_2 spacer at the incident wavelength of 435 nm which is wavelength of emission light, the diameters of Ag NPs are 20, 40, 60, 80, and 100 nm, respectively. We can find that

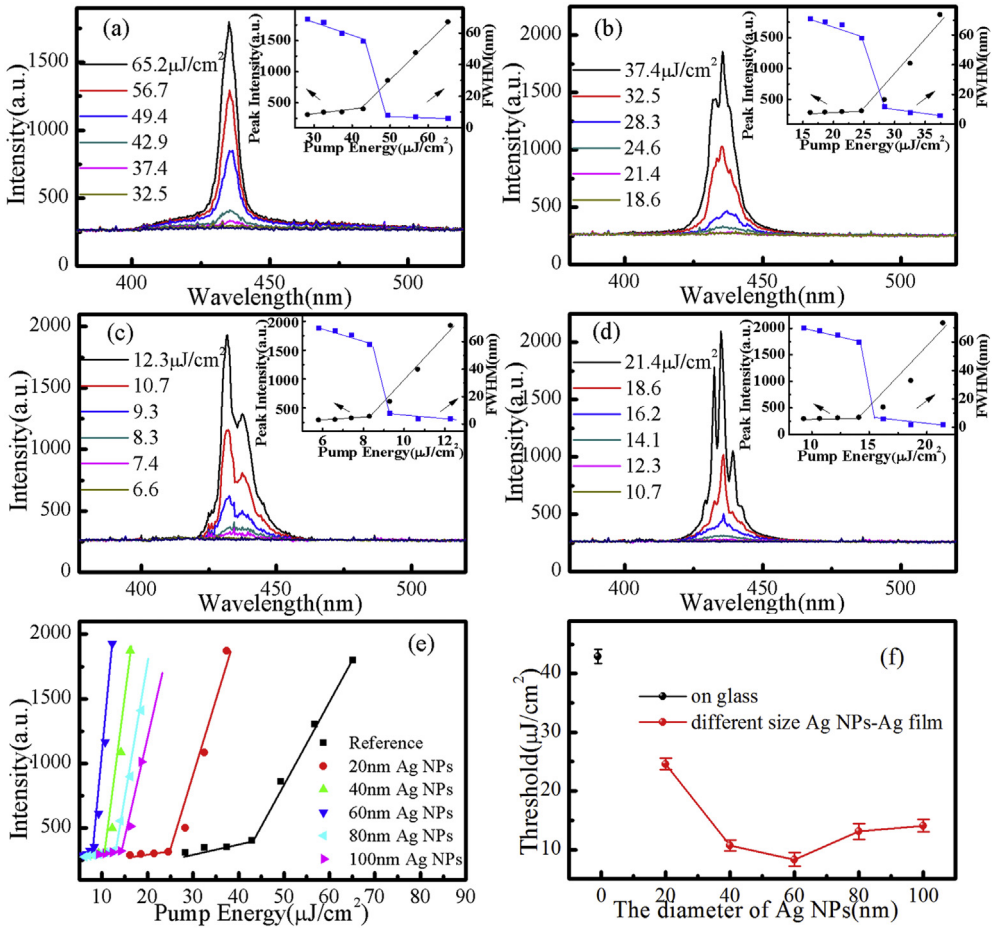

Fig. 4. The emission spectra of the devices that gain media deposited on (a) glass, (b) 20 nm, (c) 60 nm, (d) 100 nm Ag NPs-Ag film hybrid structures. The insets show the dependence of the emission intensity and the FWHM of the emission spectra on the pump intensity. For the sharp spikes of spectra appear in (b)–(d), the FWHMs above the lasing threshold were estimated from those of sharp spikes, instead of that of the broad background. (e) Dependences of the emission intensity on the pump energy intensity for devices with different structures. (f) The lasing thresholds of the gain media deposited on glass and different sizes Ag NPs-Ag film hybrid structures.

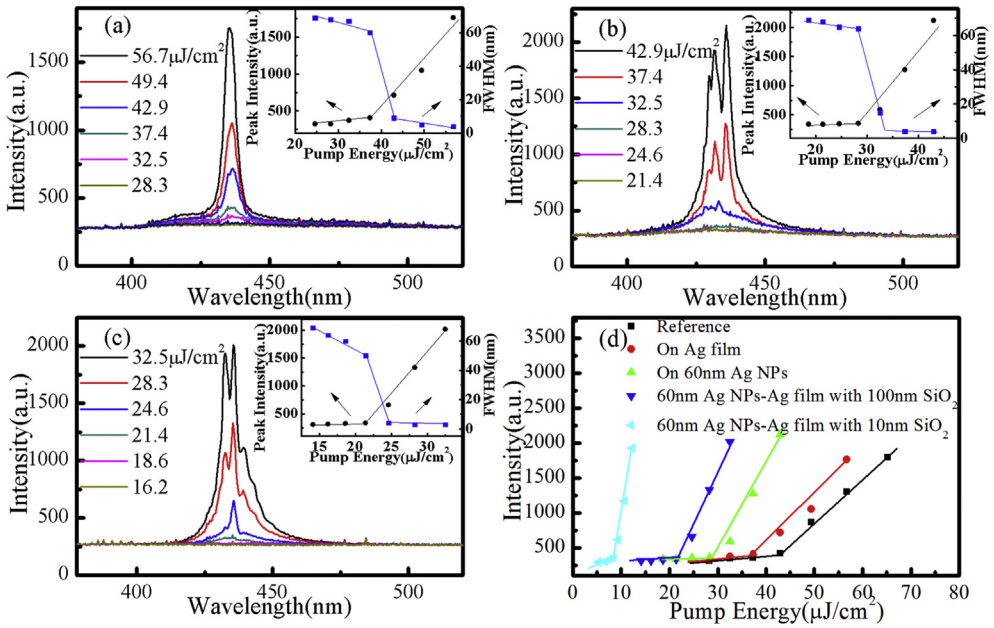

Fig. 5. The emission spectra of devices that gain media deposited on (a) Ag film, (b) 60 nm Ag NPs, (c) 60 nm Ag NPs-Ag film with 100 nm SiO_2. The insets show the emission intensity and the FWHM of the emission spectra. (d) Dependences of the emission intensity on the pump energy for different devices.

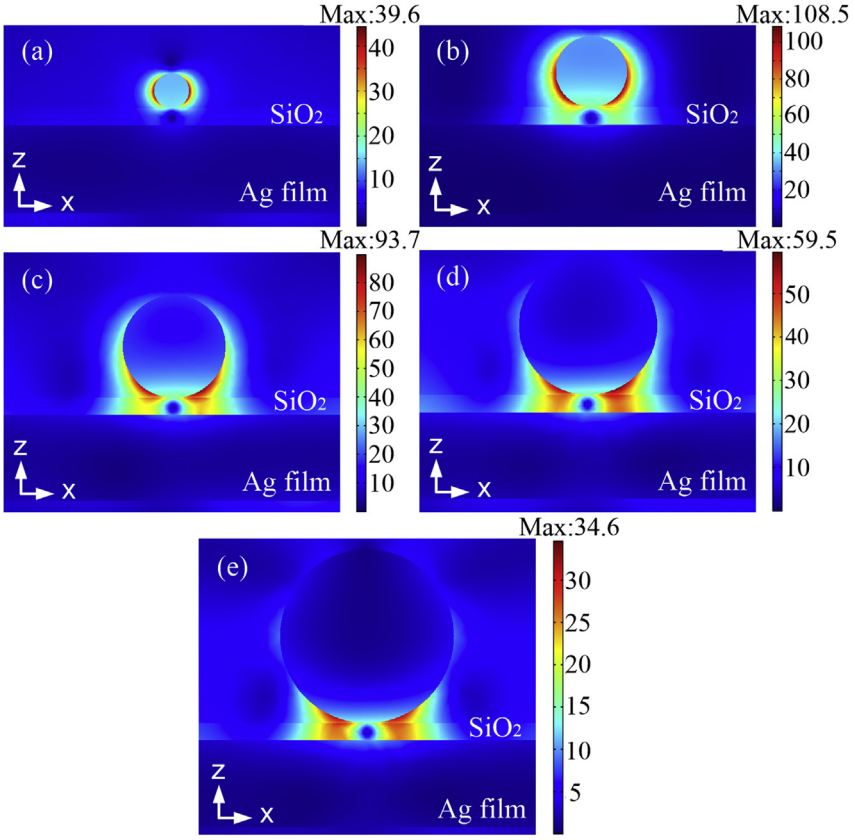

Fig. 6. The electric-field distribution of (a) 20 nm, (b) 40 nm, (c) 60 nm, (d) 80 nm, and (e) 100 nm Ag NPs-Ag film with 10 nm SiO_2 spacer.

with the increasing of Ag NPs size, the electric field intensity of hybrid structure increases at first, and then reduces, there is the strongest electric field when the diameter of Ag NPs is 40 nm. In addition, for illustrating the advantage of Ag NPs-Ag film hybrid structure on enhanced localized electric field and proving the existing of the plasmon coupling interaction between Ag NPs and Ag film, the electric field intensities of independent 60 nm Ag NPs (Fig. 7(a)) and the 60 nm Ag NPs-Ag film with 100 nm SiO_2 spacer

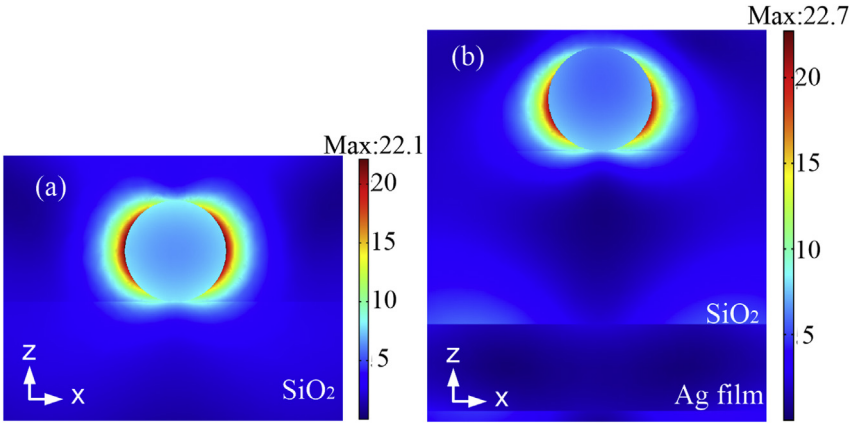

Fig. 7. The electric-field distribution of (a) 60 nm Ag NPs on SiO_2 without Ag film, (b) 60 nm Ag NPs-Ag film with 100 nm SiO_2 spacer.

(Fig. 7(b)) were also simulated. Comparing with those two structures shown in Fig. 7, we found the 60 nm Ag NPs-Ag film with 10 nm SiO_2 spacer has stronger electric field. Fig. 7 also shows that when the distance between 60 nm Ag NPs and Ag film changes to 100 nm, the electric field intensity is similar as that of independent 60 nm Ag NPs, which indicates that there is no plasmon coupling when the distance between Ag NPs and Ag film is too large. Therefore, the lasing threshold of device based on Ag NPs-Ag film hybrid structure with 100 nm SiO_2 spacer is higher than that with 10 nm SiO_2 spacer shown in Figs. 4 and 5. And the stronger localized electric field of hybrid structure due to the plasmon coupling interaction between LSPR of Ag NPs and SPP of Ag films is identified in Figs. 6 and 7.

On the other hand, to evaluate another mechanism of scattering effect of different size Ag NPs-Ag film, the scattering cross sections (σ_s) of different sizes Ag NPs at $\lambda = 435$ nm were calculated using Mie theory [29]. For comparison, $\sigma_s/V_{particle}$ was calculated as normalized scattering cross section, $V_{particle}$ is the particle volume [5,6]. Fig. 8 shows that, with the Ag NPs diameter increasing from 20 nm to 100 nm, the $\sigma_s/V_{particle}$ increases. Moreover, comparing to the Ag NPs only, the Ag NPs-Ag film has stronger scattering effect. Theoretical and experimental have already verified that the leaking photons escaping from gain medium can be reflected and reinjected into the gain media by the external feedback of metallic film [30–32]. Fig. 5 shows that the gain media deposited on hybrid structure with 100 nm SiO_2 spacer has lower lasing threshold than that deposited on separate Ag NPs, which is due to the stronger scattering by external feedback of Ag film (the electric field intensities of separate Ag NPs and hybrid structure with 100 nm SiO_2 are about the same shown in Fig. 7). And Table 1 shows that with increase of Ag NPs, the $E_{th\text{-}50nm}$ is lower, which also suggests that with the increasing of Ag NPs size, the scattering effect of hybrid structure increases.

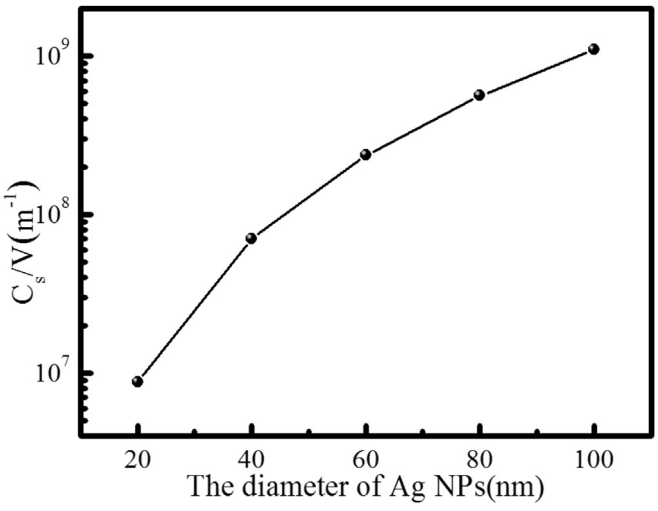

Fig. 8. The normalized scattering cross section at λ = 435 nm versus the Ag NPs size.

According to the discussion of two mechanisms about enhanced localized electric field and scattering effect of different sizes Ag NPs-Ag film hybrid structures, we can know that comparing with the independent Ag NPs or Ag film, the two mechanisms of enhanced localized electric field and scattering effect of Ag NPs-Ag film hybrid structure are all stronger, which lead to the significantly enhanced lasing. When the Ag NPs is small in hybrid structure (diameter≤40 nm), comparing to the scattering effect, the enhanced localized electric field is the dominant role to enhance lasing. With the increase of Ag NPs diameter, the scattering effect increases, the enhanced localized electric field and scattering have comparable contribution on enhancing lasing. When the size is larger (diameter ≥ 80 nm), the scattering effect is the major mechanism for enhanced lasing. And it found that there is the lowest lasing threshold in device with 60 nm Ag NPs-Ag film hybrid structure, about a factor of 5.2 times than that of reference device, both the enhanced localized electric field and scattering effect play the important role on reduction of lasing threshold. At meanwhile, the negative effect of Ag film is avoided in gain medium to realize the lower pumped threshold than that of the neat gain medium.

4. Conclusion

In summary, avoiding the negative effect of metallic film on the lasing has been an important issue for the electrical pumped laser. In this article, we investigated the lasing properties based on different sizes Ag NPs-Ag film hybrid structures, the Ag NPs diameters ranged from 20 nm to 100 nm. The lowest lasing threshold was achieved by introducing 60 nm Ag NPs-Ag film hybrid structure. Comparing to the separate Ag NPs and Ag film, the Ag NPs-Ag film hybrid structure presented the more intense local electric field due to the plasmonics coupling between the Ag NPs and the Ag film. In the meantime, the re-injection of emitted light into the organic gain media by the Ag film could also enhance scattering strength. By studying the enhanced localized electric field and the scattering effect of Ag NPs-Ag film hybrid structure in experiment and Mie theory, we found that the enhanced localized electric field

and scattering all contribute to the enhanced lasing. When the Ag NPs is small in hybrid structure (diameter≤40 nm), enhanced localized electric field is the major role for enhanced lasing; with the increase of Ag NPs size, the enhanced electric field and scattering all play the important roles on the enhanced lasing; when the size is larger (diameter≥80 nm), compared with enhanced localized electric field, the scattering effect plays a main role on the enhancement of lasing properties. The lowest lasing threshold was achieved due to both the enhanced localized electric field and scattering effect. Our results could provide us a unique idea to effectively avoid the negative effect of metallic film and realize the lower pumped threshold. This method is expected to be a potential metal-modified technology for improving the lasing performance.

Acknowledgements

This work was financially supported by National Natural Science Foundation of China (Program No. 61605105), Natural Science Basic Research Plan in Shaanxi Province of China (Program No. 2016JQ6038), Scientific Research Program Funded by Shaanxi Provincial Education Department (Program No. 16JK1085), Scientific Research Fund of Shaanxi University of Science and Technology (Program No. 2016BJ-02).

References

[1] J.R. Lakowicz, Radiative decay engineering 5: metal-enhanced fluorescence and plasmon emission, Anal. Biochem. 337 (2005) 171–194.
[2] F. Tam, G.P. Goodrich, B.R. Johnson, N.J. Halas, Plasmonic enhancement of molecular fluorescence, Nano Lett. 7 (2007) 496–501.
[3] A. Zayats, I. Smolyaninov, Near-field photonics: surface plasmon polaritons and localized surface plasmons, J. Opt. A Pure Appl. Opt. 5 (2003) S16–S50.
[4] J. Mock, R. Hill, A. Degiron, S. Zauscher, Distance-dependent plasmon resonant coupling between a gold nanoparticle and gold film, Nano Lett. 8 (2008) 2245–2252.
[5] O. Popov, A. Zilbershtein, D. Davidov, Random lasing form dye-gold nanoparticles in polymer films: enhanced at the surface-plasmon-resonance wavelength, Appl. Phys. Lett. 89 (2006), 191116–1~3.
[6] O. Popov, A. Zilbershtein, D. Davidov, Enhanced amplified emission induced by surface plasmons on gold nanoparticles in polymer film random lasers, Polym. Adv. Technol. 18 (2007) 751–755.
[7] X. Meng, K. Fujita, Y. Zong, S. Murai, Random lasers with coherent feedback from highly transparent polymer films embedded with silver nanoparticles, Appl. Phys. Lett. 92 (2008), 201112–1~3.
[8] X. Meng, K. Fujita, S. Murai, K. Tanaka, Coherent random lasers in weakly scattering polymer films containing silver nanoparticles, Phys. Chem. A 79 (2009), 053817–1~7.
[9] T. Zhai, X. Zhang, Z. Pang, X. Su, H. Liu, Li Wang, Random, Laser based on waveguided plasmonic gain channels, Nano Lett. 11 (2011) 4295–4298.
[10] E. Heydari, R. Flehr, J. Stumpe, Influence of spacer layer on enhancement of nanoplasmon-assisted random lasing, Appl. Phys. Lett. 102 (2013), 133110–1~4.
[11] J. Stehr, J. Crewett, F. Schindler, R. Sperling, A.W. Holleit-ner, A low threshold polymer laser based on metallic nanoparticle gratings, Adv. Mater. 15 (2003) 1726–1729.
[12] A. Mahfouda, A. Sarangana, T.R. Nelsonb, E.A. Blubaugh, Role of aggregation in the amplified spontaneous emission of [2-methoxy-5-(2′-ethylhexyloxy)-1, 4-phenylenevinylene] in solution and films, J. Lumin 118 (2006) 123–130.
[13] P. Andrew, G. Turnbull, Photonic band structure and emission characteristics of a metal-backed polymeric distributed feedback laser, Appl. Phys. Lett. 81 (2002) 3261–3264.
[14] M. Reufer, S. Riechel, J.M. Lupton, J. Feldmann, Low-threshold polymeric distributed feedback lasers with metallic contacts, Appl. Phys. Lett. 84 (2004) 3261–3264.
[15] B. Zhang, Y. Hou, Z. Lou, Y. Wang, Improvement of amplified spontaneous emission performance of conjugated polymer waveguides with a low loss cladding, Appl. Phys. Lett. 101 (2012), 153305–1~4.
[16] C. Ma, S. Liu, Effect of metal cladding thickness on guided-mode optical characteristics for metal-clad four-layer waveguides, J. Opt. Soc. Am. A 7 (1990) 1577–1581.
[17] N. Tessler, Laser based on semiconducting organic materials, Adv. Mater. 11 (1999) 363–370.
[18] B. Villers, B.J. Schwartz, Destruction of amplified spontaneous emission via chemical doping at low-work-function metal/conjugated polymer interfaces, Appl. Phys. Lett. 90 (2007), 091106–1~3.
[19] Y. Wan, Z. Guo, X. Jiang, K. Fang, J. Quasi-spherical silver nanoparticles: aqueous synthesis and size control by the seed-mediated Lee-Meisel method, Colloid Interface Sci. 394 (2013) 263–268.
[20] K. Aslan, Z. Leonenk, Annealed silver-island films for applications in metal-enhanced fluorescence: interpretation in terms of radiating plasmons, J. Fluoresc. 15 (2005) 643–654.
[21] L. Ma, Z. Wu, S. Ning, Theoretical insight into the deep-blue amplified spontaneous emission of new organic semiconductor molecules, Org. Electron 15 (2014) 3144–3153.
[22] H. Yang, S. Yu, J. Yan, L. Zhang, Random lasing action from randomly assembled ZnS nanosheets, Nanoscale Res. Lett. 5 (2010) 809–812.
[23] F. Li, O. Solomesch, P. Mackie, D. Cupertino, Low gain threshold of the cavity mode close to the cutoff wavelength in a three-slab asymmetric conjugated polymer-based waveguide structure, J. Appl. Phys. 99 (2006), 013101–1~4.
[24] S. Ning, X. Zhao, H. Dong, L. Ma, X. Hou, Enhancement of amplified spontaneous emission in organic gain media by the metallic film, Org. Electron 15 (2014) 2052–2058.
[25] M.A. Díaz-García, F. Hide, M.R. Andersson, Plastic lasers: semiconducting polymers as a new class of solid-state laser materials, Synth. Met. 84 (1997) 455–462.
[26] X. Zhao, Z. Wu, S. Ning, S. Liang, D. Wang, Xun Hou, Random lasing from granular surface of waveguide with blends of PS and PMMA, Opt. Express 19 (2011) 16126–16131.
[27] Q. Song, L. Wang, S. Xiao, X. Zhou, L. Liu, L. Xu, Random laser emission from a surface-corrugated waveguide, Phys. Rev. B 72 (2005), 035424–1~4.
[28] X. Meng, K. Fujita, S. Murai, T. Matoba, K. Tanaka, Plasmonically controlled lasing resonance with metallic-dielectric core-shell nanoparticles, Nano Lett. 11 (2011) 1374–1378.
[29] C.F. Bohren, D.R. Huffman, Absorption and Scattering of Light by Small Particles, Wiley, New York, 1998, p. 83. Chap. 4.
[30] C. Dominguez, R. Maltez, Dependence of random laser emission on silver nanoparticle density in PMMA films containing rhodamine 6G, J. Opt. Soc. Am. B 28 (2011) 1118–1123.
[31] P. Oliveira, J. McGreevy, N. Lawandy, External-feedback effects in high gain scattering media, Opt. Lett. 22 (1997) 895–897.
[32] H. Cao, Y. Zhao, Effect of external feedback on lasing in random media, Appl. Phys. Lett. 75 (1999) 1213–1215.